AFRL-RX-WP-TP-2012-0412

VACUUM LEVELS NEEDED TO SIMULATE INTERNAL FATIGUE CRACK GROWTH IN TITANIUM ALLOYS AND NICKEL-BASE SUPERALLOYS: THERMAODYNAMIC CONSIDERATIONS (PREPRINT)

J.M. Larsen
Metals Branch
Structural Materials Division

V. Sinha
UES, Inc.

AUGUST 2012
Interim

STINFO COPY

AIR FORCE RESEARCH LABORATORY
MATERIALS AND MANUFACTURING DIRECTORATE
WRIGHT-PATTERSON AIR FORCE BASE, OH 45433-7750
AIR FORCE MATERIEL COMMAND
UNITED STATES AIR FORCE

REPORT DOCUMENTATION PAGE

1. REPORT DATE *(DD-MM-YY)*	2. REPORT TYPE	3. DATES COVERED *(From - To)*
August 2012	Technical Paper	1 July 2012 – 1 August 2012

4. TITLE AND SUBTITLE	
VACUUM LEVELS NEEDED TO SIMULATE INTERNAL FATIGUE CRACK GROWTH IN TITANIUM ALLOYS AND NICKEL-BASE SUPERALLOYS: THERMAODYNAMIC CONSIDERATIONS (PREPRINT)	**5a. CONTRACT NUMBER** In-house
	5b. GRANT NUMBER
	5c. PROGRAM ELEMENT NUMBER 62102F

6. AUTHOR(S)	
J.M. Larsen (AFRL/RXCM) V. Sinha (UES, Inc.)	**5d. PROJECT NUMBER** 4347
	5e. TASK NUMBER 20
	5f. WORK UNIT NUMBER X071

7. PERFORMING ORGANIZATION NAME(S) AND ADDRESS(ES)	8. PERFORMING ORGANIZATION REPORT NUMBER
Metals Branch Structural Materials Division 2230 Tenth Street Wright-Patterson AFB, OH 45433-7750	AFRL-RX-WP-TP-2012-0412

9. SPONSORING/MONITORING AGENCY NAME(S) AND ADDRESS(ES)	10. SPONSORING/MONITORING AGENCY ACRONYM(S)
Air Force Research Laboratory Materials and Manufacturing Directorate Wright-Patterson Air Force Base, OH 45433-7750 Air Force Materiel Command, United States Air Force	AFRL/RXCM
	11. SPONSORING/MONITORING AGENCY REPORT NUMBER(S) AFRL-RX-WP-TP-2012-0412

12. DISTRIBUTION/AVAILABILITY STATEMENT
Approved for public release; distribution unlimited. Preprint to be submitted to Metallurgical and Materials Transactions A.

13. SUPPLEMENTARY NOTES
This work was funded in whole or in part by Department of the Air Force In house. The U.S. Government has for itself and others acting on its behalf an unlimited, paid-up, nonexclusive, irrevocable worldwide license to use, modify, reproduce, release, perform, display, or disclose the work by or on behalf of the U.S. Government. PA Case Number and clearance date: 88ABW-2012-1792, 27 March 2012. This document contains color.

14. ABSTRACT
Prior studies have examined fatigue growth of surface cracks in vacuum to simulate sub-surface growth in Ti-alloys and Ni-base superalloys. Even with the highest vacuum level attained using "state-of-the-art" pumps, it is unclear if conditions of internal crack growth are truly simulated. We consider thermodynamics of the oxidation process to help answer this question. This consideration helps explain a previously reported anomalous behavior of longer life in air than in vacuum under certain material/ test conditions.

15. SUBJECT TERMS
Titanium alloy, Ni-base superalloys, Internal Cracks, Fatigue Crack Growth, Equilibrium Oxygen Pressure, Ellingham-Richardson Diagram

16. SECURITY CLASSIFICATION OF:			17. LIMITATION OF ABSTRACT:	NUMBER OF PAGES	19a. NAME OF RESPONSIBLE PERSON (Monitor)
a. REPORT Unclassified	**b. ABSTRACT** Unclassified	**c. THIS PAGE** Unclassified	SAR	20	Andrew Rosenberger **19b. TELEPHONE NUMBER** *(Include Area Code)* N/A

Vacuum Levels Needed to Simulate Internal Fatigue Crack Growth in Titanium Alloys and Nickel-base Superalloys: Thermodynamic Considerations

V. Sinha[1,2] and J.M. Larsen[1]

[1]Air Force Research Laboratory, Materials and Manufacturing Directorate, AFRL/RXLM
Wright-Patterson Air Force Base, OH 45433, USA

[2]UES, Inc., 4401 Dayton-Xenia Road, Dayton, OH 45432, USA

Abstract

Prior studies have examined fatigue growth of surface cracks in vacuum to simulate sub-surface growth in Ti-alloys and Ni-base superalloys. Even with the highest vacuum level attained using "state-of-the-art" pumps, it is unclear if conditions of internal crack growth are truly simulated. We consider thermodynamics of the oxidation process to help answer this question. This consideration helps explain a previously reported anomalous behavior of *longer* life in air than in vacuum under certain material/ test conditions.

Keywords: Titanium alloy, Ni-base superalloys, Internal Cracks, Fatigue Crack Growth, Equilibrium Oxygen Pressure, Ellingham-Richardson Diagram
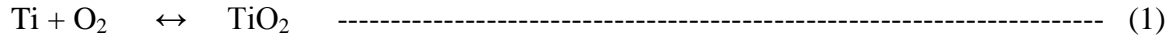
In aircraft turbine engine rotors, cracks may grow under conditions of variable temperature, frequency, hold-time, stress-ratio and stress level. Cumulative-damage models for life prediction need to account for all these variables, as well as interaction effects [1]. A major challenge for improved life management within the framework of a damage-tolerant approach involves the phenomenon of *internal* fatigue crack growth that is observed in many materials, including Ti-alloys and Ni-base superalloys. There is a need to better measure internal fatigue crack growth rates (FCGR, *i.e. da/dN*) and to better understand the micromechanisms of such crack growth. Examples of internal cracking in Ti-alloys include fatigue cracking at sub-surface hard α (HA) defects [2], as well as initiation and growth under cyclic and dwell-time fatigue, with resultant formation of sub-surface crystallographic facets [3-8]. Examples of internal cracking in Ni-base superalloys include subsurface crystallographic fatigue crack initiation and initiation from nonmetallic inclusions in René 88DT at 593 $^\circ$C [9-12]. In this material, internal cracking occurred by localization of cyclic plastic deformation on {111} slip planes in the region close to and parallel to twin boundaries in favorably oriented large grains [12]. Internal crack initiation was also reported at nonmetallic inclusions or large defects in high strength Ni-base superalloys at elevated temperatures (650 $^\circ$C and 760 $^\circ$C) and at low strain-ranges [13-15].

Measurements of internal FCGR (usually in the small-crack regime) are inherently difficult, because direct observations of these cracks are not possible. Determinations of FCGR on internal cracks are also difficult with conventional techniques, such as electric potential-drop and compliance methods. Since an important difference between the internal cracks and surface cracks is that the former are not exposed to air, several studies have examined the fatigue growth of surface cracks in vacuum to simulate the growth of internal cracks [2, 9, 10, 16]. This approach assumes that tests in vacuum (pressures as low as 3×10^{-10} torr, *i.e.* 4×10^{-8} Pa have been employed) avoid the formation of any oxide layer on freshly formed surfaces with advance of the crack-front, and thereby adequately mimic the conditions of internal crack growth. The current paper examines the validity of this assumption in the context of prior studies of environmental effects on fatigue behavior and thermodynamics of oxidation process. Ti-alloys are considered first, followed by a discussion on Ni-base superalloys.

Prior studies on effects of environment on fatigue behavior of Ti-alloys have primarily focused on room-temperature response, and a summary is provided in Table I. Although contributions of mechanisms such as specimen heating and the role of moisture were invoked to rationalize the effects of vacuum on FCGR, the role of oxygen via adsorption and oxide formation on the freshly formed fracture surfaces is a major contributor to the observed differences in *da/dN* under different environments [18, 20]. Any oxide on the freshly formed surface will limit reverse slip at the crack-tip during the unloading portion of a fatigue cycle [18], and thereby lead to a higher FCGR. To attain higher reverse slip akin to the conditions of sub-surface crack growth, the oxide formation needs to be completely avoided. We believe that the thermodynamics of the oxidation process needs to be considered to determine the conditions under which oxide formation may be fully avoided. From the fatigue response for the investigated range of vacuum levels, it was suggested [2, 16, 17, 20] that air pressures $< 1.33 \times 10^{-4}$ Pa capture the full vacuum effects (*i.e.* no Ti-oxidation). In prior studies, thermodynamic considerations were not presented of the equilibrium oxygen partial pressure (p_{O_2}), below which oxidation of titanium is energetically unfavorable. In the current work, we have employed an Ellingham-Richardson diagram [21-25] to determine this equilibrium p_{O_2} necessary to preclude oxidation of pristine crack surfaces.

The maximum use temperature for α/β and near-α titanium alloys in aircraft engine applications is ~400 $^\circ$C and ~600 $^\circ$C, respectively [26]. Therefore, temperatures from room-temperature to 600 $^\circ$C are relevant for the current discussion on Ti-alloys. Ellingham [21] plotted ΔG^0 (standard free energy of formation of oxides) *versus T* (absolute temperature) for a series of metals. To facilitate the determination of equilibrium p_{O_2} at any given temperature T, Richardson and Jeffes [22] added a nomographic scale to the Ellingham diagram. The Ellingham-Richardson diagram for a series of oxides is shown in Fig. 1. For any oxidation reaction, the value of equilibrium p_{O_2} at temperature T_1 is read off the diagram as that value on the nomographic scale, which is collinear with the points $\Delta G^0 = 0$, $T = 0$ and $\Delta G^0_{T_1}$ (for oxidation reaction under consideration), $T = T_1$.

The Ti-oxidation reaction is:

$$Ti + O_2 \quad \leftrightarrow \quad TiO_2 \qquad \text{---} \quad (1)$$

To determine the equilibrium p_{O_2} at 300 $^\circ$C (573 K), a straight line is drawn through points $\Delta G^0 = 0$, $T = 0$ and $\Delta G^0_{573\,K}$ (for Ti-oxidation), $T = 573$ K. The straight line cuts the Richardson nomographic scale at $p_{O_2} \approx 10^{-75}$ atm $= 10^{-70}$ Pa. Therefore, to avoid oxidation at 300 $^\circ$C of freshly formed titanium fracture surfaces and truly simulate the conditions of subsurface cracking, the p_{O_2} should be $< 10^{-70}$ Pa. At $p_{O_2} > 10^{-70}$ Pa, the oxide is more stable than titanium at 300 $^\circ$C and therefore, oxidation cannot be avoided. A similar consideration shows that a $p_{O_2} < 10^{-41}$ Pa at 600 $^\circ$C and a $p_{O_2} < 10^{-155}$ Pa at room-temperature would be required for eliminating oxide formation.

Fig. 1 depicts the case of oxidation of pure Ti into its pure oxide (TiO_2) and facilitates determination of equilibrium p_{O_2} at $a_{Ti} = a_{TiO_2} = 1$, where a_{Ti} and a_{TiO_2} are activities of Ti and TiO_2, respectively. However, for the case of a Ti-alloy, $a_{Ti} < 1$, and for the general case of formation of a solid solution of oxides, $a_{TiO_2} < 1$. Compared to the case of $a_{Ti} = a_{TiO_2} = 1$, $a_{Ti} < 1$ results in an increase in the slope of *ΔG-T* line, whereas $a_{TiO_2} < 1$ results in a decrease (Fig. 2). This change in slope affects the equilibrium p_{O_2} for Ti-oxidation: $p_{O_2(a_{Ti} < 1)}$ is higher than $p_{O_2(a_{Ti} = 1)}$ and $p_{O_2(a_{TiO_2} < 1)}$ is lower than $p_{O_2(a_{TiO_2} = 1)}$. The expressions for equilibrium $p_{O_2(a_{Ti} < 1)}$ and equilibrium $p_{O_2(a_{TiO_2} < 1)}$ are as follows [27]:

$$\text{At a fixed } T \text{ and } a_{TiO_2} = 1, \quad p_{O_2(a_{Ti} < 1)} = \frac{p_{O_2(a_{Ti} = 1)}}{a_{Ti}} \qquad \text{------------------------------------} \quad (2)$$

and at a fixed T and $a_{Ti} = 1$, $p_{O_2(a_{TiO_2} < 1)} = a_{TiO_2} \times p_{O_2(a_{TiO_2} = 1)}$ --------------------- (3)
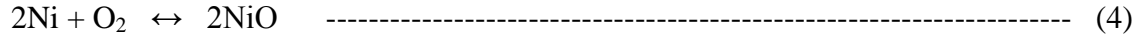
For both Ti-6Al-4V and Ti-6Al-2Sn-4Zr-2Mo, the mole-fraction of Ti in the alloy (X_{Ti}) is 0.86. At this high X_{Ti}, the behavior can be assumed to follow Raoult's law, and a_{Ti} can be approximated as [28]: $a_{Ti} \approx X_{Ti}$. Using equation (2) at 300 $^\circ$C, $p_{O_2(a_{Ti} = 0.86)} = \frac{10^{-70}}{0.86} = 1.16 \times 10^{-70}$

3

Pa and at 600 $^{\circ}$C, $p_{O_2(a_{Ti}=0.86)} = \frac{10^{-41}}{0.86} = 1.16 \times 10^{-41}$ Pa. Thus, a consideration of non-unit a_{Ti} leads to a minor change in equilibrium p_{O_2} and the conclusions described above remain unchanged. In a general case, TiO$_2$ will be formed in a solution of oxides. However, a non-unit a_{TiO_2} will lead to a lower equilibrium p_{O_2} for Ti-oxidation and therefore, it is not considered in the current study with an aim to determine the upper limit of equilibrium p_{O_2}.

An ultra-high-vacuum chamber with the "state-of-the-art" pumps can achieve a pressure as low as 4×10^{-8} Pa [2], *i.e.* $p_{O_2} = 0.21 \times 4 \times 10^{-8} = 8.4 \times 10^{-9}$ Pa, as air consists of ~ 21 vol% oxygen. It is clear from prior studies that a significant change in FCGR and crack growth mechanism occurs with a change of vacuum level in the investigated range (10^5 to 4×10^{-8} Pa). Since p_{O_2} needed to completely avoid oxide formation on freshly formed fracture surfaces is orders of magnitude lower than 8.4×10^{-9} Pa, it is plausible that further changes in FCGR and crack growth mechanisms would occur if it were possible to run tests at p_{O_2} that are less than the equilibrium p_{O_2} for Ti-oxidation reaction. A possible approach to attain these extremely low p_{O_2} could be *via* use of a metal that has a lower ΔG^0 than Ti. One such metal is aluminum (Fig. 1). By placing the Ti-specimen inside an Al-enclosure (without making any physical contact) and keeping the complete configuration in an ultra-high-vacuum chamber, it may be possible to attain levels of p_{O_2}, where Ti is more stable than TiO$_2$ and therefore, its oxidation can be avoided. This will help attain conditions akin to subsurface cracking. To increase the kinetics of Al-oxidation, and thereby to reach the desired p_{O_2} in a shorter time, the surface-area to volume ratio of enclosure can be increased (*e.g. via* use of Al-foam) and prior to the fatigue test, the whole assembly can be heated to a moderate temperature (*e.g.* 400 $^{\circ}$C) that is too low to cause any microstructural modifications in Ti-alloys. It is also interesting to note that to prevent Al-oxidation at room-temperature, a $p_{O_2} < 10^{-175}$ Pa will be needed (Fig. 1). This equilibrium p_{O_2} is orders of magnitude lower than that for Ti-oxidation. It follows that the experiments in ultra-high-vacuum chamber ($p_{O_2} = 8.4 \times 10^{-9}$ Pa) cannot truly simulate the internal fatigue crack growth in Al-alloys.

Thermodynamic consideration of oxidation process is now extended to Ni-base superalloys. Current Ni-base superalloys can withstand service temperatures as high as ~ 1100 $^{\circ}$C, and are extensively used in the combustor and turbine sections of aircraft engines [29, 30]. Therefore, temperatures from room-temperature to 1100 $^{\circ}$C are relevant for the current discussion on Ni-base superalloys. A summary of prior investigations on effects of environment on fatigue behavior of several different Ni-base superalloys is provided in Table II. Oxidation greatly influences the fatigue fracture mechanisms in Ni-base superalloys, and thereby causes a variation in FCGR, as well as crack-initiation under different environments. In general, a higher FCGR and a shorter fatigue life were observed in air than in vacuum [31-34]. This normal behavior is depicted schematically in Fig. 3(a). However, an anomalous behavior was reported in one study, where fatigue life in air was longer than that in vacuum at 927 $^{\circ}$C [35]. This anomalous behavior is shown schematically in Fig. 3(b). The conditions for subsurface-cracking in air and surface-cracking in vacuum are assumed to be the same in ref. [35], and it is difficult to explain the observed anomalous behavior with this assumption. A consideration of thermodynamics of oxidation process in the current study shows that the conditions for subsurface-cracking in air and surface-cracking in vacuum are actually different, and this can help explain the observed anomalous behavior in ref. [35].

The Ni-oxidation reaction is:

$$2Ni + O_2 \leftrightarrow 2NiO \quad \text{--} \quad (4)$$

From the thermodynamic considerations (Fig. 1), it is clear that oxidation of pure Ni at 927 $^\circ$C cannot be avoided at $p_{O_2} > 10^{-11}$ atm (10^{-6} Pa). Activity of Ni (a_{Ni}) in Ni-base superalloys is less than unity, which results in a higher equilibrium p_{O_2} than for the case of pure Ni, $i.e.$ $a_{Ni} = 1$ (Fig. 2). An expression similar to equation (2) can be written to determine equilibrium $p_{O_2(a_{Ni}<1)}$:

$$\text{At a fixed } T \text{ and } a_{NiO} = 1, \; p_{O_2(a_{Ni}<1)} = \frac{p_{O_2(a_{Ni}=1)}}{(a_{Ni})^2} \quad \text{-------------------------------------} \quad (5)$$

The denominator in the right-hand-side of equation (5) has $(a_{Ni})^2$ whereas in equation (2) it is a_{Ti}. This difference of square arises because 2 moles of Ni react with 1 mole of oxygen (equation (4)), and only 1 mole of Ti reacts with 1 mole of oxygen (equation (1)). A non-unit a_{NiO} will result in a lower equilibrium p_{O_2} for Ni-oxidation (Fig. 2), and this case is not considered in the current study with an aim to determine the upper limit of equilibrium p_{O_2}.

The mole-fraction of Ni (X_{Ni}) in Mar-M200 is 0.61 and assuming Ni to follow Raoult's law in Mar-M200, $a_{Ni} \approx X_{Ni} = 0.61$. Therefore, from equation (5), the equilibrium $p_{O_2(a_{Ni}=0.61)} = \frac{10^{-6}}{0.37} = 2.7 \times 10^{-6}$ Pa. It follows that at the vacuum levels of 6.65×10^{-4} - 1.6×10^{-3} Pa ($i.e.$ $p_{O_2} = 1.4 \times 10^{-4}$ - 3.4×10^{-4} Pa), employed in the work of Duquette and Gell [35], the oxidation of freshly formed fatigue fracture surfaces does occur. On the other hand, during the internal crack initiation and growth for tests in air, this oxidation is not feasible. From these considerations, it is expected that there is a lower level of reverse slip at the crack-tip during unloading portion of a fatigue cycle in vacuum than in air, because the dominant cracks are surface-initiated in vacuum and subsurface-initiated in air. This can explain the reported higher life in air than in vacuum at 927 $^\circ$C. At the intermediate temperatures of 427-760 $^\circ$C, the kinetics of oxidation are expected to be slower than at 927 $^\circ$C, and this possibly can account for similar fatigue lives in air and in vacuum at 427-760 $^\circ$C that was reported in ref. [35].

At 700 $^\circ$C, a $p_{O_2} < 10^{-16}$ atm (10^{-11} Pa) is needed to completely avoid oxidation of Ni (Fig. 1). At lower temperatures, even a lower p_{O_2} will be required. When the crack is surface-connected in both air and vacuum, lower fatigue lives and higher FCGR were observed in air than in vacuum (Fig. 3(a)) [31-34]. In these prior studies [31-34], air pressures $\gg 5 \times 10^{-11}$ Pa ($i.e.$ $p_{O_2} \gg 10^{-11}$ Pa) in vacuum tests and temperatures < 700 $^\circ$C were used. Therefore, oxidation of grain boundaries, freshly formed fracture surfaces or slip surfaces cannot be completely avoided during vacuum tests under these conditions. However, the level of oxidation is expected to be more in air than in vacuum, and this causes a lower life/ higher FCGR in air. On the other hand, when crack initiates internally in air and at surface in vacuum [35], the oxidation of internal crack surfaces (air test) is completely avoided, and it cannot be avoided for surface cracks (vacuum test). This results in a longer life in air than in vacuum under these conditions at a high temperature of 927 $^\circ$C (Fig. 3(b)).

The environmentally-enhanced crack growth during sustained-load tests at elevated temperatures of Ni-base superalloys is reported to occur by stress-assisted diffusion of oxygen ahead of crack-tip, and the subsequent selective oxidation of Ti, Al, Cr and Nb [36]. This is consistent with thermodynamic considerations, since lines for oxidation of Al, Ti, Nb and Cr are below that of Ni in Fig. 1. Assuming similar selective oxidation of Ti, Al, Cr and Nb during a fatigue test, it is evident that even a lower p_{O_2} will be needed to completely avoid oxidation of a Ni-base superalloy than determined from the consideration of Ni-oxidation alone (Fig. 1).

To assess the bonding of oxide to Ti-alloys and Ni-base superalloys, a consideration of Pilling-Bedworth ratio (PBR) is useful. PBR is defined as the volume ratio of oxide and metal from which the oxide forms [37-39]. A PBR < 1 results in a discontinuous oxide layer, whereas a PBR > 2 may cause spalling due to large compressive stresses in the oxide layer [38]. A PBR = 1-2 may be associated with a continuous and adherent oxide layer. For TiO_2/Ti and NiO/Ni systems, PBR = 1.76 and 1.70, respectively [24]. Hence, a continuous and adherent oxide layer is expected for both the systems. This is supported by the experimental observations of an adherent oxide on Ti-6Al-4V at 600 $^{\circ}$C [40], on pure Ni at 600-1200 $^{\circ}$C [41] and on Ni-base superalloys at 1100 $^{\circ}$C [42]. Moreover, only a strongly-bonded oxide layer at the pristine fracture surface can influence the fatigue behavior of Ti-alloys and Ni-base superalloys in a manner summarized in Tables I and II. Therefore, we believe that the oxide formed at the new fracture surfaces in Ti-alloys and Ni-base superalloys is indeed adherent and stable.

References:

1. J.M. Larsen and T. Nicholas, Engineering Fracture Mechanics, Vol. 22, No. 4, pp. 713-730, 1985.

2. R.C. McClung, B.H. Lawless, M. Gorelik, C. Date, Y. Gill, R.S. Piascik, in: Fatigue Behavior of Titanium Alloys, R.R. Boyer, D. Eylon and G. Lütjering (eds.), TMS, pp. 211-218, 1999.

3. V. Sinha, J.E. Spowart, M.J. Mills, and J.C. Williams, Metallurgical and Materials Transactions A, vol. 37A, pp. 1507-1518, 2006.

4. V. Sinha, M.J. Mills, and J.C. Williams, Metallurgical and Materials Transactions A, vol. 35A, pp. 3141-3148, 2004.

5. M.R. Bache, W.J. Evans, and H.M. Davies: J. Mater. Sci., 1997, vol. 32, pp. 3435-42.

6. M.R. Bache, H.M. Davies, and W.J. Evans: *Titanium '95: Science and Technology*, University Press, Cambridge, U.K., 1995, pp. 1347-54.

7. V. Sinha, M.J. Mills, and J.C. Williams, Journal of Materials Science, vol. 42, no. 19, pp. 8334-8341, 2007.

8. V. Sinha, M.J. Mills, and J.C. Williams, Metallurgical and Materials Transactions A, vol. 37A, pp. 2015-2026, 2006.

9. S.K. Jha, M.J. Caton, J.M. Larsen, and A.H. Rosenberger, K. Li, and W.J. Porter, in: Materials Damage Prognosis, J.M. Larsen, L. Christodoulou, J.R. Calcaterra, M.L. Dent, M.M. Derriso, W.J. Hardman, J.W. Jones, and S.M. Russ, Eds., TMS, Warrendale, PA, 2005, pp. 343-350.

10. M. J. Caton, S. K. Jha, A. H. Rosenberger, and J. M. Larsen, in: Superalloys 2004, K.A. Green, T.M. Pollock, H. Harada, T.E. Howson, R.C. Reed, J.J. Schirra, and S. Walston, Eds., TMS, Warrendale, PA, 2004, 305-312.

11. A. Shyam, C. J. Torbet, S. K. Jha, J. M. Larsen, M. J. Caton, C. J. Szczepanski, T. M. Pollock, and J. W. Jones, in: Superalloys 2004, K.A. Green, T.M. Pollock, H. Harada, T.E. Howson, R.C. Reed, J.J. Schirra, and S. Walston, Eds., TMS, Warrendale, PA, 2004, 259-268.

12. J. Miao, T.M. Pollock and J.W. Jones, Acta Materialia 57 (2009) pp. 5964–5974.

13. J.M. Hyzak and I.M. Bernstein, Metallurgical Transactions, Vol. 13A, pp. 33-43, 1982.

14. J.M. Hyzak and I.M. Bernstein, Metallurgical Transactions, Vol. 13A, pp. 45-52, 1982.

15. J. Gayda and R. V. Miner, Int J Fatigue, Vol 5, No 3, July 1983, pp. 135-143.

16. P. E. Irving and C. J. Beevers, Metallurgical Transactions, vol. 5, pp. 391-398, 1974.

17. D. M. James: RAE Technical Memorandum CPM 66, October 1966.

18. M. Sugano, S. Kanno and T. Satake, Acta Metallurgica, Vol. 37, No. 7, pp. 1811-1820, 1989.

19. S. Adachi, L. Wagner and G. Lütjering: *Proceedings of International Conference on Fatigue of Engineering Materials and Structures*, The Institution of Mechanical Engineers, Sheffield, UK, 1986, pp. 67-74.

20. M.R. Bache, W.J. Evans and M. McElhone, Materials Science and Engineering A234-236 (1997) pp. 918-922.

21. H.J.T. Ellingham, J. Soc. Chem. Ind., **63**: 125 (1944).

22. F.D. Richardson and J.H.E. Jeffes, J. Iron and Steel Inst., **160**: 261 (1948).

23. D.R. Gaskell, Introduction to Metallurgical Thermodynamics, Fifth edition, Taylor and Francis Group, New York, NY, USA, p. 359, 2008.

24. Z. Grzesik, in: ASM Handbook, vol. 13 A, Corrosion: Fundamentals, Testing and Protection, S.D. Cramer and B.S. Covino, Jr., Volume Eds., ASM International, Materials Park, OH, USA, pp. 92-94, 2003.

25. N. Birks, G.H. Meier, and F.S. Pettit, Introduction to the High-Temperature Oxidation of Metals, Second Edition, Cambridge University Press, Cambridge, UK, pp. 22-24, 2006.

26. R. Boyer, G. Welsch and E.W. Collings, Materials Properties Handbook: Titanium Alloys, ASM International, Materials Park, OH, USA, pp. viii-ix, 1994.

27. D.R. Gaskell, Introduction to Metallurgical Thermodynamics, Fifth edition, Taylor & Francis Group, New York, NY, USA, pp. 387-388, 2008.

28. D.R. Gaskell, Introduction to Metallurgical Thermodynamics, Fifth edition, Taylor & Francis Group, New York, NY, USA, pp. 215-216, 2008.

29. R.C. Reed, The Superalloys: Fundamentals and Applications, Cambridge University Press, New York, USA, pp. 3-5, 2006.

30. T.M. Pollock and S. Tin, Journal of Propulsion and Power, Vol. 22, No. 2, March-April 2006, pp. 361-374.

31. J. P. Pédron and A. Pineau, Materials Science and Engineering, 56 (1982) 143 - 156.

32. C. Laird and G.C. Smith, Philosophical Magazine, vol. 8, issue 95, pp. 1945-1963, Nov. 1963.

33. H. H. Smith and P. Shahinian, Transactions of the ASM, Volume 62, pp. 549-551, 1969.

34. D.J. Duquette and M. Gell, Metallurgical Transactions, Volume 2, pp. 1325-1331, 1971.

35. D.J. Duquette and M. Gell, Metallurgical Transactions, Volume 3, pp. 1899-1905, 1972.

36. C.F. Miller, G.W. Simmons, and R.P. Wei, Scripta Materialia 48 (2003) 103–108.

37. N.B. Pilling and R.E. Bedworth, Journal of the Institute of Metals, Vol. 29, pp. 529-591, 1923.

38. M.G. Fontana, Corrosion Engineering, Third edition, McGraw-Hill Book Company, New York, NY, USA, pp. 505-506, 1986.

39. H.H. Uhlig and R.W. Revie, Corrosion and Corrosion Control: An Introduction to Corrosion Science and Engineering, Third edition, John Wiley & Sons, New York, NY, USA, p. 190, 1985.

40. S. Frangini, A. Mignone and F. De Riccardis, Journal of Materials Science, Vol. 29, pp. 714-720, 1994.

41. Y.Y. Liu and K. Natesan, in: Adhesion in Solids, D.M. Mattox, et al., Eds., Materials Research Society Symposium Proceedings, Vol. 119, MRS, Pittsburgh, PA, USA, pp. 213-221, 1988.

42. E. Fedorova, D. Monceau and D. Oquab, Corrosion Science 52 (2010) 3932–3942.

Table I: Summary of Prior Studies of Environmental Effects on Room-Temperature Fatigue Behavior in Ti-alloys

Reference	Material Examined	Environment	Fatigue Response	Conclusions and Proposed Mechanisms, relevant for Current Study
McClung, *et al.*, [2]	(i) Ti-6Al-4V (ii) Ti-6Al-2Sn-4Zr-2Mo+Si	Vacuum level[a]: 1.33×10^{-2} to 1.33×10^{-7} Pa (10^{-4} to 10^{-9} torr)	(a) No variation in *near-threshold* FCGR between 1.33×10^{-4} and 1.33×10^{-7} Pa, whereas it was clearly higher at 1.33×10^{-3} Pa. (b) Similar FCGR between 1.33×10^{-3} and 1.33×10^{-7} Pa in *Paris regime*, whereas it was 2× higher at 1.33×10^{-2} Pa.	Vacuum levels better (less) than 1.33×10^{-4} Pa should be adequate to capture full vacuum effects.
		Vacuum level: better (less) than 1.33×10^{-5} Pa	(a) Similar FCGR for air and vacuum in the *upper Paris regime*, but a considerably lower FCGR for vacuum in the *near-threshold regime*. (b) A significantly higher ΔK_{th} in vacuum than in air.	
James [17], as discussed by Irving and Beevers [16]	Ti-5Al-2.5Sn	Vacuum levels: 1.33×10^{-3} Pa and 4×10^{-6} Pa, with L_{N_2}[b] cold traps to reduce water vapor content at both vacuum levels	Identical FCGR at the two vacuum levels investigated.	A vacuum of 1.33×10^{-3} Pa plus a cold trap was below the critical pressure for titanium at room temperature
Irving and Beevers [16]	Ti-6Al-4V	Vacuum level: 1.33×10^{-3} Pa, with L_{N_2} cold trap	(a) A marginally (~ 3-4×) lower FCGR for vacuum than for air in the *Paris* regime, but at least 3-orders of magnitude lower FCGR for vacuum than for air in the *near-threshold* regime. (b) A significantly higher ΔK_{th} in vacuum than in air.	

[a]Since air consists of ~ 21 vol% oxygen, the vacuum level (air pressure) needs to be multiplied by 0.21 to determine the corresponding partial pressure of oxygen (p_{O_2}). For example, under atmospheric conditions $p_{O_2} = 0.21$ atm (2.1×10^4 Pa), and a vacuum level of 1.33×10^{-2} Pa corresponds to a p_{O_2} of 2.8×10^{-3} Pa.

[b]L_{N_2}: Liquid Nitrogen

Table I (Contd.)

Reference	Material Examined	Environment	Fatigue Response	Conclusions and Proposed Mechanisms, relevant for Current Study
Sugano, *et al.*, [18]	Pure Ti	Vacuum level: As low as 1.33×10^{-3} Pa	A sharp increase in fatigue life for pressure reduction from 10 Pa to 1 Pa, which was attributed to the enhanced plasticity leading to crack tip blunting at air pressures $\leq$ 1 Pa.	The enhanced plasticity was caused by internal (frictional) heating of the specimen during fatigue testing in vacuum, which, in turn, results from reduced heat transfer to the surrounding atmosphere due to paucity of gas molecules at pressures $\leq$ 1 Pa.
Adachi, *et al.*, [19]	Ti-6Al-4V	Vacuum level: better (less) than 10^{-4} Pa	A significantly higher fatigue strength in vacuum than in air.	
Bache, *et al.*, [20]	Ti-6Al-4V	Vacuum level: 1.33 Pa to 1.33×10^{-4} Pa	Similar FCGR under atmospheric conditions and intermediate vacuum of 1.33 Pa, whereas significantly lower FCGR at 1.33×10^{-4} Pa. This reduction in *da/dN* was more significant in the near-threshold regime.	
		$p_{H_2}{}^c$ = 13.3 Pa and $p_{Ar}{}^d$ = 13.3 Pa	FCGR is slightly *lower* in hydrogen than in air. The FCGR in hydrogen and argon are similar.	Hydrogen does not cause a higher FCGR, even though it is considered a detrimental species in the water vapor model.
	Ti-6Al-4V with oxygen contents from 900 to 5100 ppm	Air	A significant increase in FCGR, especially in the near-threshold regime, on increasing the internal oxygen-content from its nominal value of ~ 2000 ppm to 5100 ppm.	Oxygen plays a major role in influencing the FCGR response.

^{c} p_{H_2}: partial pressure of hydrogen

^{d} p_{Ar}: partial pressure of argon

Table II: Summary of Prior Studies of Environmental Effects on Fatigue Behavior in Ni-base Superalloys

Reference	Material/ Temperature Examined	Environment	Fatigue Response	Conclusions and Proposed Mechanisms, relevant for Current Study
Gayda and Miner [15]	Astroloy, Waspaloy, MERL 76, NASA II-B7 René 95, and IN100/ 650 °C	Air	A dwell at the maximum load results in an increase in FCGR and this increase is more pronounced for higher strength/ finer grain alloys.	(a) The rapid intergranular crack growth due to grain boundary oxidation, which is accelerated by a finer grain size and a tensile dwell. (b) A change in the crack growth mode of fine-grain IN100 from transgranular to intergranular at the point where internally initiated fatigue crack grew to break through the surface with the concomitant exposure of crack-tip to the outside air.
Pédron and Pineau [31]	IN718/ 650 °C	Vacuum level: better (less) than 1.33×10^{-3} Pa	(a) A substantially higher FCGR in air than in vacuum. Frequency affected the FCGR and fracture mode in air, but not in vacuum. (b) FCGR under dwell-fatigue conditions is essentially microstructure-insensitive in vacuum, whereas it is strongly microstructure-sensitive in air with a substantially higher FCGR for a fine-grain microstructure than for a coarse-grain one.	(a) Oxidation plays an important role in fatigue response of Ni-base superalloys. (b) Operating mechanism is grain boundary oxidation and resultant embrittlement in air, which is expected to be more severe for a finer grain microstructure.
Laird and Smith [32]	Pure Ni/ Room Temperature	Vacuum level: 6.65×10^{-3} Pa	A longer life in vacuum than in air, especially at low stress-ranges.	Air enhances crack growth via chemical attack at the crack-tip.
Smith and Shahinian [33]	Inconel X-750/ 500 °C	Oxygen pressure of 133 Pa and vacuum level of 8×10^{-5} Pa	A higher FCGR and a lower life in oxygen than in vacuum.	Finer slip bands produced in oxygen result from oxidation of freshly exposed slip surfaces and cause early crack initiation/ faster FCGR.

Table II (contd.)

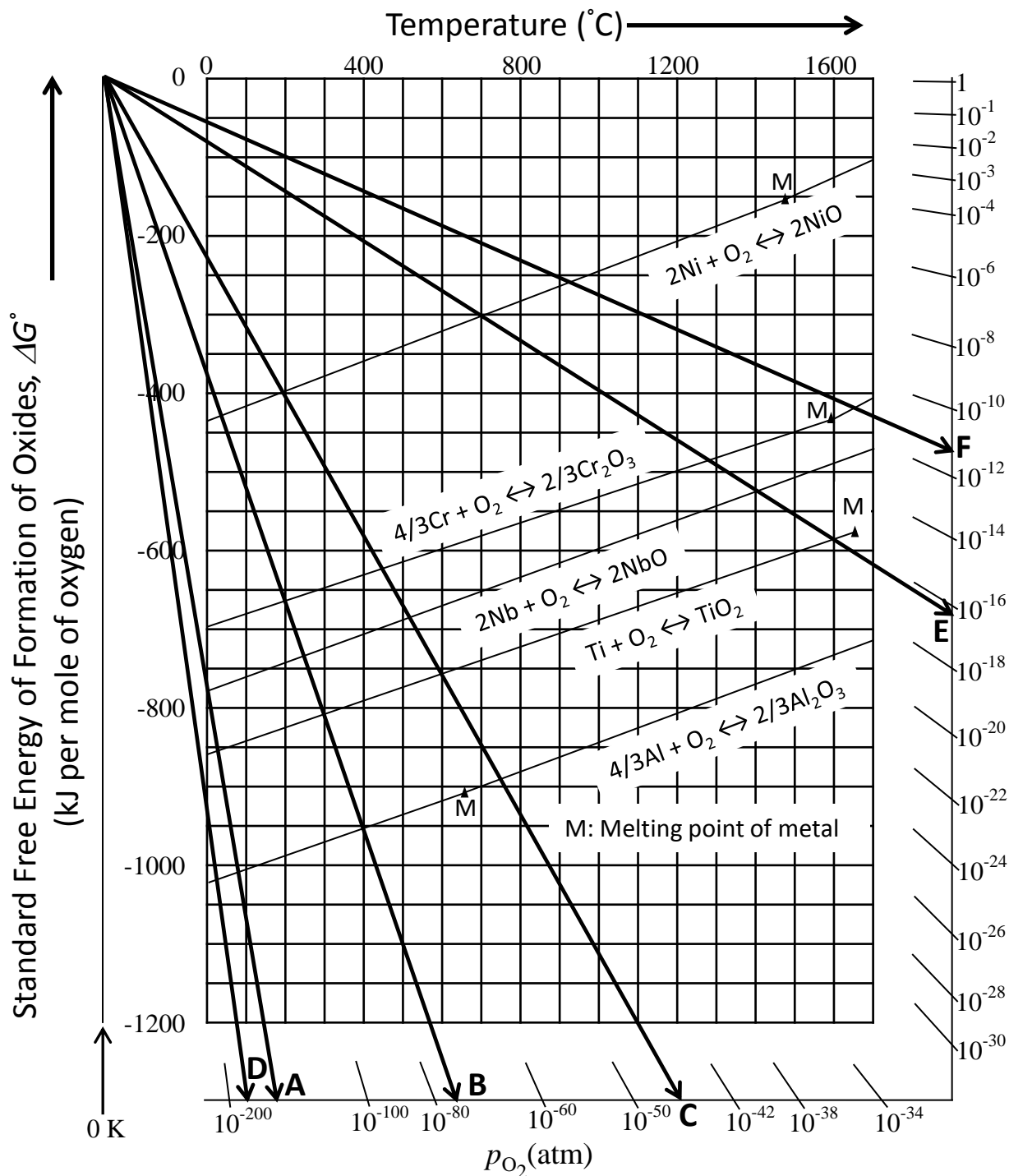| Reference	Material/ Temperature Examined	Environment	Fatigue Response	Conclusions and Proposed Mechanisms, relevant for Current Study
Duquette and Gell [34]	Single crystal Mar-M200/ Room Temperature	Vacuum level: 1.6×10^{-3} to 6.65×10^{-4} Pa	Fatigue life was significantly higher in vacuum than in air, and the difference in life increased with a reduction of stress-range.	(a) *Surface-initiation* of cracks from casting micropores in both air and vacuum. (b) Oxygen adsorption at the crack-tip in air resulted in a change of fracture mechanism and a lower life/ higher FCGR. (c) At low stress-ranges, crack propagation mechanism is ductile-rupture in vacuum and cyclic-cleavage in air.
		Dry, humidified, and normal laboratory air	Fatigue life and fracture surface appearances are the same in dry, humidified and normal laboratory air.	Oxygen, rather than water vapor, adsorbed at the crack-tip resulted in higher FCGR and cleavage fracture at low stress-ranges.
Duquette and Gell [35]	Single crystal Mar-M200/ 427-927 °C	Vacuum level: 1.6×10^{-3} to 6.65×10^{-4} Pa	(a) Fatigue lives are similar in air and vacuum at temperatures 427-760 °C. (b) At 927 °C, the fatigue life in air is surprisingly *greater* than that in vacuum.	(a) *Surface-initiation* of cracks in vacuum and *subsurface-initiation* in air at 427-927 °C. (b) Crack initiation at the casting micropores in both air and vacuum at 427-927 °C.

Fig. 1: Ellingham-Richardson diagram for oxidation reactions (after ref. [21-25]). The equilibrium oxygen pressure for Ti-oxidation is determined at room-temperature, 300 °C and 600 °C: labeled "A", "B" and "C", respectively; it is determined for Al-oxidation at room-temperature: labeled "D", and for Ni-oxidation at 700 °C and 927 °C : labeled "E" and "F", respectively.

Fig. 2: Variation in ΔG vs. T line for non-unit activities of metal (M) and its oxide (MO_2 or MO). For the case of Ti-oxidation, oxide is of type MO_2 and for Ni-oxidation, oxide is of type MO. At a fixed temperature T_1, the equilibrium p_{O_2} for oxidation reaction is denoted on the nomographic scale by point "A" for the case of $a_M = a_{MO_2}$ or $a_{MO} = 1$, by point "B" for the case of $a_M < 1$ and a_{MO_2} or $a_{MO} = 1$, and by point "C" for the case of $a_M = 1$ and a_{MO_2} or $a_{MO} < 1$. Here, a_M and (a_{MO_2} or a_{MO}) stand for activities of metal and its oxide, respectively. After ref. [27].
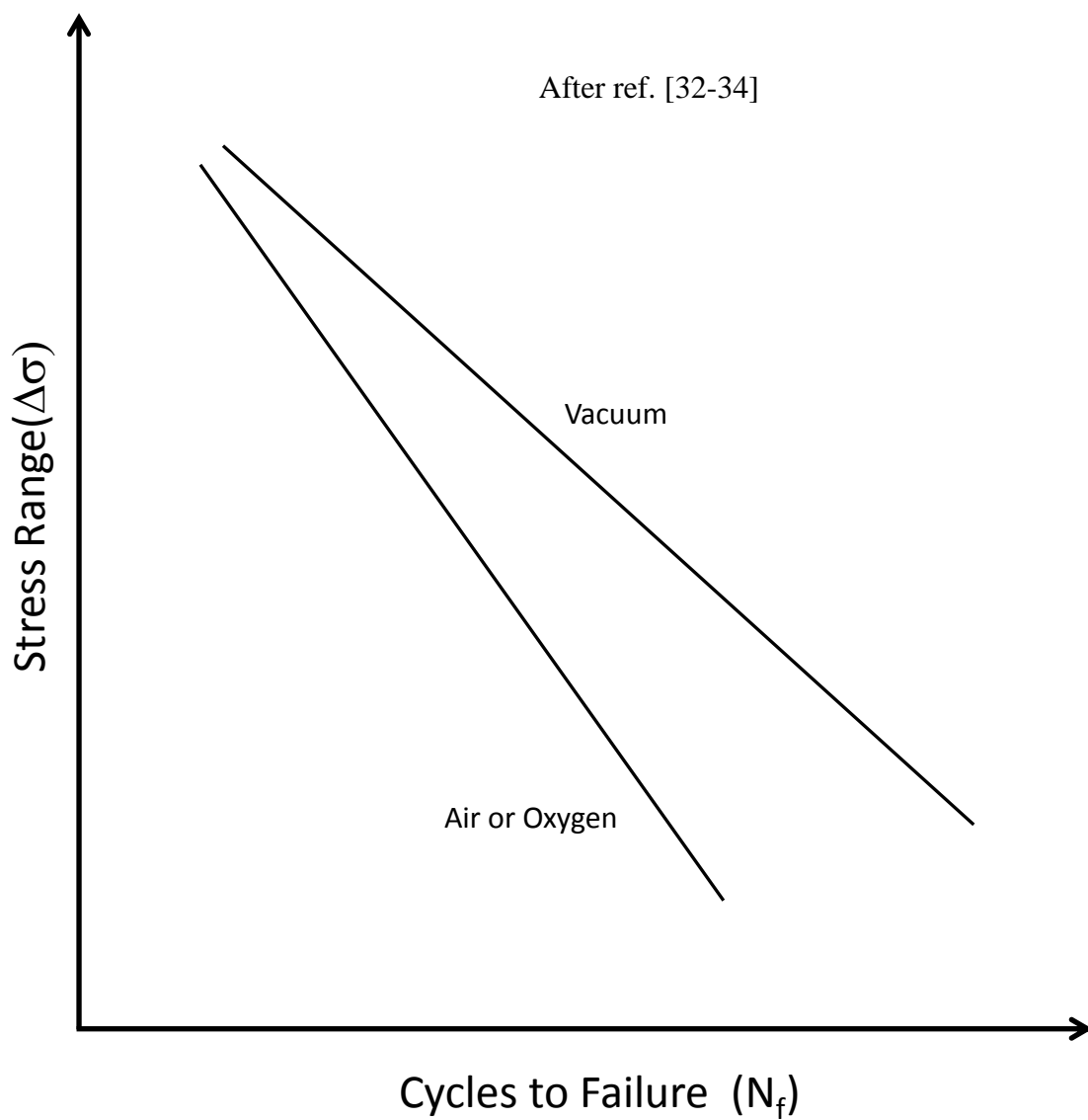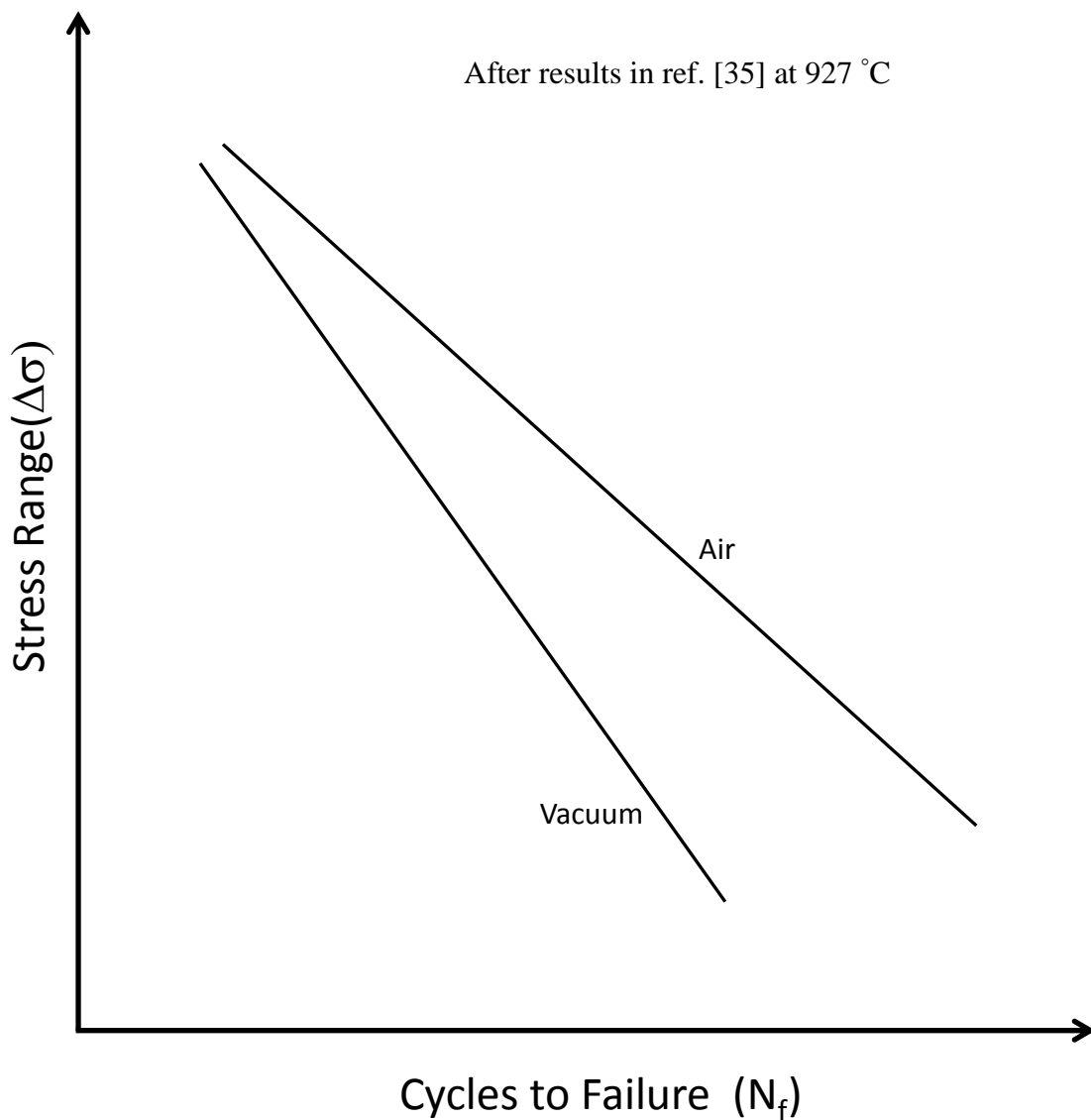
Fig. 3(a)

After results in ref. [35] at 927 °C

(b)

Fig. 3: Schematics of (a) *normal* and (b) *anomalous* fatigue response with the change of environment. The normal behavior is manifested by a *longer* fatigue life in vacuum than in air/ oxygen, whereas the anomalous behavior is manifested by a *shorter* fatigue life in vacuum than in air. (a) is for the condition of surface-cracking in both air/ oxygen and vacuum, and (b) is for the condition of subsurface-cracking in air and surface-cracking in vacuum.